ChemComm

COMMUNICATION

View Article Online
View Journal | View Issue

Cite this: *Chem. Commun.*, 2017, 53, 12020

Received 9th August 2017,
Accepted 7th October 2017

DOI: 10.1039/c7cc06209e

rsc.li/chemcomm

Polymer-mediated metallophilic interactions for gram-scale production, high-yield (~90%) synthesis of ultrathin bismuth nanowires†

Tzu-Lun Kao and Hsing-Yu Tuan *

High-yields (~90%) of ultrathin (<4 nm) bismuth nanowires (Bi UNWs) were obtained by reducing the polymeric strands of oleylamine-bismuth 2-ethylhexanoate complexes formed *via* metallophilic interactions with the mediation of a copolymer (PVP–HDE).

Nanowires with diameters below 10 nm were mostly considered as ultrathin nanowires (UNWs), however, interest in even thinner nanowires having diameters below 2 nm has grown greatly owing to the intriguing properties they possibly possess, especially quantum conductance and ballistic conduction.[1,2] Theoretically, the decrease in the diameter of nanowires can enhance the colloidal stability and lead to various beneficial effects on sensors and catalyst applications.[3,4]

In the past few years, UNWs have been obtained through different approaches, including templating,[5,6] ligand-control,[7,8] and oriented attachment.[9,10] The general idea of templating is to use materials with specific structures as a mold to restrict the crystal growth, followed by the removal of the template to obtain UNWs.[1] For instance, the Li group employed an anodic alumina membrane (AAM) as a template along with pulsed electrochemical deposition to synthesize Bi UNW arrays.[11] However, the drawbacks are low yield with template residues due to impurities and the lack of colloidal stability. With respect to ligand-control, the anisotropic lattice growth was induced by the coverage of surfactants on specific crystal planes.[12] Qian synthesized Cu_2S UNWs with a diameter of 1.7 nm, by employing 1-dodecanethiol and oleic acid as the ligand mixture.[13] Oriented attachment is another effective way to produce UNWs,[14] and it represents the phenomenon in which specific crystal planes of nanoparticles attach to each other to prevent the high surface energy crystal planes from reaching equilibrium when the system energy is too high.[12] PbSe UNWs synthesized *via* oriented attachment by Murray *et al.* showed colloidal stability and monodispersity from the predetermined size.[15]

Recently, a new synthetic approach toward ultrathin nanowires was employed using metallophilic interactions, which falls under the templating category.[1] Metallophilic interactions result due to the attractive forces between metals, which exist in noble or heavy metals, including gold and bismuth.[16–18] These metal elements tend to string together in series and form a 1D structure due to their metallophilic interactions, which was followed by *in situ* reduction and led to the formation of ultrathin nanowires. For example, syntheses of gold ultrathin nanowires were performed by allowing a gold precursor to react with oleylamine. In this case, the metallophilic interactions are called aurophilic interactions.[19,20] The gold precursor formed complexes with oleylamine, and then a 1D structure, which was called polymeric strands by Korgel and Xia, was formed due to the aurophilic interactions, and then after reduction gold ultrathin nanowires were formed.[20]

In this work, we report a facile synthesis of Bi UNWs with a diameter ranging from 2–4 nm in a solution-phase system simply by heating the mixture of bismuth 2-ethylhexanoate and oleylamine in the presence of a copolymer (polyvinylpyrrolidone–hexadecane, PVP–HDE), which led to high-yields (~90%) of Bi UNWs. Fig. 1 shows the schematic illustration of the growth mechanism of Bi UNWs, which indicates that bismuth 2-ethylhexanoate and oleylamine formed polymer strands due to the metallophilic interactions of bismuth, followed by *in situ* reduction in the presence of the copolymer (PVP–HDE) for hindering the growth of Bi particles, which resulted in high yields of Bi UNWs. A gram-scale synthesis experiment was also conducted to assess the possibility of Bi UNWs for industrial scale production by increasing the amounts of reactants, showing excellent results for Bi UNWs with good quality and high yield.

Fig. 2(a) and (b) shows the scanning electron microscopy (SEM) images of well-interlaced Bi ultrathin nanowires (Bi UNWs) at different magnifications, and the bundle-like mesostructure was immediately recognized (see more SEM images in Fig. S1 (ESI†) and the TEM image in Fig. S2, ESI†). Although the exact diameter cannot be measured from these images, it is obvious that the diameter of the wires is less than 10 nm especially

Department of Chemical Engineering, National Tsing Hua University, Hsinchu 30013, Taiwan. E-mail: hytuan@che.nthu.edu.tw

† Electronic supplementary information (ESI) available. See DOI: 10.1039/c7cc06209e

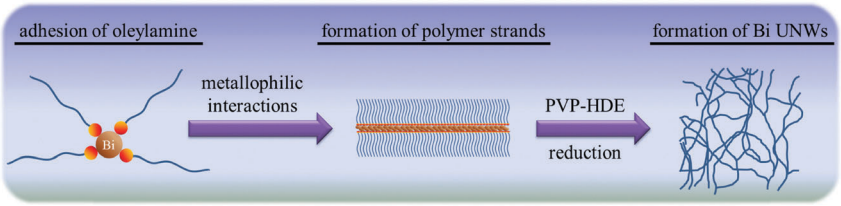

Fig. 1 Schematic illustration of the growth mechanism of Bi UNWs.

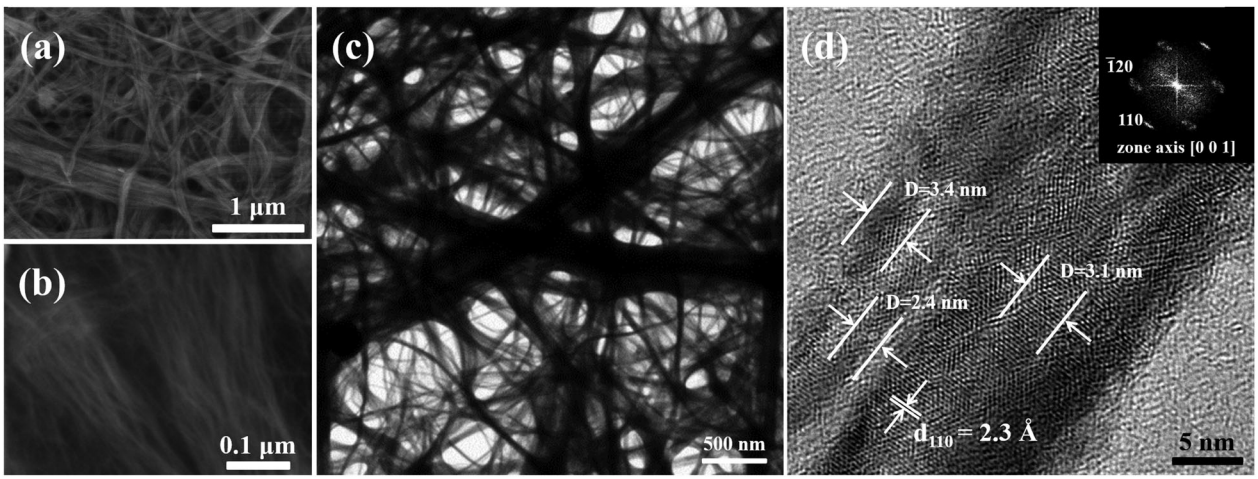

Fig. 2 (a and b) SEM images, at different magnifications, of the Bi UNWs obtained by reacting 0.64 g bismuth 2-ethylhexanoate in 10 ml oleylamine in the presence of 2 g PVP–HDE at 200 °C for 30 min. (c) The TEM image of the as-synthesized Bi UNWs, (d) the HRTEM image of the bismuth UNWs with the diameter of some wires measured in nm and the corresponding FFT pattern shown in the inset.

where the arrows point out in Fig. S1(e) and in Fig. S2 (ESI†). The crystallinity of the Bi UNWs was tested by means of X-ray diffraction (XRD) as shown in Fig. S3(a) (ESI†), indicating that the peaks corresponding to different crystal planes were in good agreement with the Bi rhomb-centered structure (JCPDS No. 85-1329). The simulated Bi unit cell shown in Fig. S3(b) (ESI†) was obtained by utilizing the software Crystal Maker Ver. 2.2.4 along with the information provided by the XRD database JCPDS No. 85-1329, including the space group and cell parameters. Furthermore, the single crystal diffraction pattern of rhomb-centered Bi was then simulated. Bi UNWs with a diameter range of 2 to 4 nm were observed as shown in Fig. 2(c) and (d). The inset of Fig. 2(d) shows the corresponding FFT which is in accordance with the previously simulated single crystal diffraction pattern with the [0 0 1] zone axis, indicating that the Bi UNWs grew along the [1 1 0] direction with a *d*-spacing of 2.3 Å, which coincided with the (110) lattice plane spacing of 2.27 Å listed in JCPDS No. 85-1329.[21] Also, a melting phenomenon of Bi UNWs was observed (Fig. S4(a) and (b), ESI†) due to the low melting point, which was probably lower than that of bulk Bi (~271 °C), resulting from the surface effect.[22,23] The Bi UNWs melted under electron beam irradiation, which led to the formation of small liquid droplets of Bi followed by re-crystallization into polycrystalline nanowires during TEM examination (Fig. S4(c) and (d), ESI†).[24,25] Despite the obstacle caused due to the melting of bismuth, with our relentless effort, we are still able to acquire TEM images that are sufficient for the measurement of the diameter of Bi UNWs (Fig. S5 and S6, ESI†), which clearly show sub-five nanometer Bi UNWs.

To better understand how the Bi UNWs were formed, specimens were sampled at different stages of the reaction in a typical synthesis for TEM and XPS analysis to observe the growth of Bi UNWs. Fig. 3(a)–(c) shows the TEM images of the product obtained once the temperature reached 120 °C, 150 °C, and was maintained at 200 °C for 30 minutes, respectively. The gradual formation of Bi UNWs was instantly observed. The corresponding XPS spectra are shown in Fig. 3(d). Analysis of these spectra was done by following procedures including the calibration of the binding energy by C 1s (284.8 eV) and the curve fitting which was done using the software XPSPEAK Ver. 4.1. The Bi 4f peaks in curve I were located at 164.2 eV and 158.9 eV, showing the primary presence of Bi^{3+} when sampled, once the temperature reached 120 °C.[26,27] In curve II, a different set of Bi 4f peaks located at 161.8 eV and 156.5 eV appeared when sampled, once the reaction temperature reached 150 °C, indicating that Bi^{3+} was reduced to Bi^{0} gradually, and finally, the Bi 4f peaks shown in curve III were merely located at 161.8 eV and 156.5 eV, indicating pure elemental bismuth,[26,28] which was in good agreement with the previous studies of the synthesis of Au UNWs.[19,20] Also, the XRD spectrum of the as-synthesized Bi UNW gel collected by centrifugation (Fig. 3(e)) showed periodic peaks with a constant spacing of ~2.1°, which was similar to the XRD spectrum of the Au^{+} complex gel

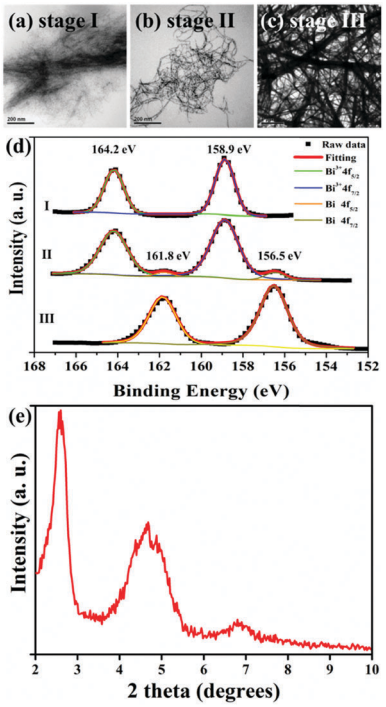

Fig. 3 TEM images of the product sampled during the heating process from room temperature to 200 °C in a one batch experiment: (a) at the moment the temperature reached 120 °C; (b) at the moment the temperature reached 150 °C; (c) kept at 200 °C for 30 minutes. (d) XPS spectra with I–III curves corresponding to the TEM images (a–c). (e) The XRD spectrum of the as-synthesized Bi UNWs gel collected by centrifugation.

prepared by continuously stirring the mixture of 0.2 mmol gold(III) chloride trihydrate and 20 ml oleylamine at room temperature for 2 days (Fig. S7, ESI†), indicating well-aligned bismuth mesostructure like Au UNWs.[19] However, the disparity between bismuth and gold assemblies in the wire-to-wire distance was probably due to the structural complexity of the precursor we employed (bismuth 2-ethylhexanoate) being distinctly higher than that of gold(I) chloride or gold(III) chloride trihydrate, hence the shift of each diffraction peak compared to that shown in Fig. S7 (ESI†) and those literature studies reporting Au UNWs.[19,20] As to the role of the copolymer (PVP–HDE) in the synthesis of Bi UNWs, different amounts of PVP–HDE were used to manifest the importance of this copolymer for a high yield of Bi UNWs. Fig. 4 shows the TEM images of Bi UNWs obtained using 0 g, 0.1 g, and 2 g of copolymer in the synthesis, respectively. Many large Bi particles were observed in the product obtained using 0 g of copolymer in the synthesis (Fig. 4(a)) while almost no particles were seen in the other two cases, indicating that the copolymer (PVP–HDE) played the role of a particle growth inhibitor, which was in agreement with many studies of syntheses of various nanoparticles by employing PVP–HDE which most likely causes steric hindrance and restrains the growth of the nanoparticles.[29–31] However, increasing the amount of copolymer did not result in any obvious difference, which indicated the limitation of the effect of the copolymer, and 0.1 g of copolymer would be sufficient for the typical synthesis of Bi UNWs. Moreover, another conclusion

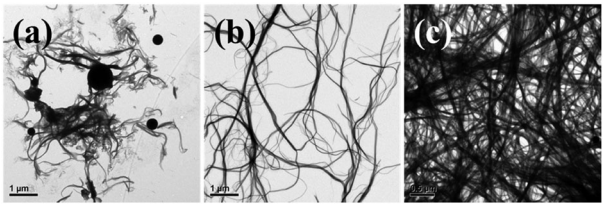

Fig. 4 (a–c) TEM images of the corresponding product resulting from the synthesis applying (a) 0 g copolymer, (b) 0.1 g copolymer, (c) 2 g copolymer at 200 °C for 30 minutes.

could be drawn from this series of experiments that the formation of particles and Bi UNWs are competing reactions, and the employment of PVP–HDE would suppress the particle growth, leading to the dominance of Bi UNWs. Therefore, the growth mechanism of Bi UNWs was concluded as follows. Oleylamine (OLA) served as the solvent and reducing agent and formed polymer strand complexes with bismuth 2-ethylhexanoate. Followed by the *in situ* reduction of Bi^{3+} to Bi^0 in the presence of the copolymer (PVP–HDE) as the particle growth inhibitor, high-yields of Bi UNWs were obtained.

A series of experiments were carried out to study how other experimental factors would affect the resulting product, including the reaction temperature and the species of reducing agent. As to the reaction temperature, the most important experimental factor of any synthesis, three syntheses were carried out at room temperature, 200 °C, and 250 °C with the reaction time fixed at 30 minutes. However, the reaction rate was too slow to form enough Bi UNWs for characterization when the experiment was carried out at room temperature; therefore, the corresponding reaction time shown in Fig. S8(a) (ESI†) was extended to 24 hours, and the resulting product shown in this TEM image was similar to that shown in Fig. 3(a), which means that the Bi became wire-like even at a low reaction temperature. However, large Bi particles appeared in the product with high reaction temperatures (Fig. S8(c), ESI†), which could be due to the higher reaction temperature, leading to the formation of crystal nuclei and growth dominating the competition reaction with the polymeric strand route, hence the large Bi particles. Fig. S9(a) and (b) (ESI†) shows the TEM images of Bi synthesized with oleylamine (OLA) and trioctylamine (TOA), respectively, resulting in tremendously different morphologies. By using OLA as the solvent and reducing agent Bi UNWs could be obtained as mentioned above. In the other case, large Bi particles could be synthesized by replacing OLA with TOA. This difference was probably due to the two amines with different structures and due to no formation of polymeric strands. Though the carbon chain of OLA (18 C) is longer than that of TOA (8 C), TOA is still considered to have a higher degree of steric hindrance due to the tertiary nature compared to OLA, which is a primary amine.[32] The steric hindrance prevented TOA from densely capping over the surfaces of particles, which resulted in a weaker surfactant and larger particles.

There were literature studies reporting the synthesis of 1D bismuth nanomaterials at a scale of tens of milligrams.[33,34] However, these syntheses either involved highly toxic

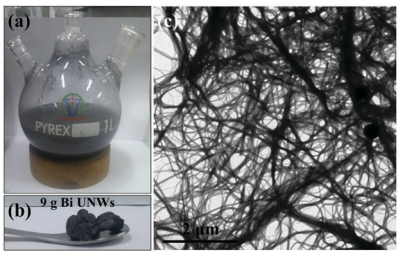

Fig. 5 (a) Photograph of the Bi UNWs synthesized in gram-scale inside a 1 liter three-necked flask, (b) photograph of purified and dried Bi UNWs and (c) the TEM image of the as-synthesized Bi UNWs in gram-scale synthesis.

N,*N*-dimethylformamide (DMF) or resulted in thick nanowires (~40 nm) or lots of nanoparticles as impurity. On the other hand, we carried out gram-scale synthesis of Bi UNWs by utilizing fifty times the amount of the chemicals in a 1 liter reactor to evaluate the possibility for industrial scale production. The photographs of the as-synthesized Bi UNWs are shown in Fig. 5(a) and (b), it is worth mentioning that 9 g of Bi UNWs were obtained in one batch with an extremely high yield of around 90% with almost no particles observed in the product. The corresponding TEM image and XRD spectrum are shown in Fig. 5(c) and Fig. S10 ESI,† indicating that the shape, monodispersity, and the crystallinity still remained the same as those of typical synthesis, which implied that this synthetic procedure had the potential to be used in the industrial scale production of Bi UNWs.

In conclusion, bismuth ultrathin nanowires (Bi UNWs) with a 2–4 nm diameter range were successfully grown in a solution-phase system following the mechanism in which oleylamine, which served as the solvent and reducing agent, formed complexes with bismuth 2-ethylhexanoate, and then the polymer strands were formed owing to the metallophilic interactions of bismuth, followed by *in situ* reduction in the presence of a copolymer (PVP–HDE) as a particle growth inhibitor to obtain a high yield of Bi UNWs. A gram-scale synthesis experiment was also carried out, showing a remarkable result of 9 g Bi UNWs obtained in one batch synthesis with good quality and a high yield of ~90%.

H.-Y. Tuan acknowledges the financial support from the Ministry of Science and Technology through the grants of NSC 102-2221-E-007-023-MY3, MOST 103-2221-E-007-089-MY3, MOST 103-2622-E-007-025 and MOST 102-2633-M-007-002.

Conflicts of interest

There are no conflicts to declare.

Notes and references

1 L. Cademartiri and G. A. Ozin, *Adv. Mater.*, 2009, **21**, 1013–1020.
2 J. I. Pascual, J. Méndez, J. Gómez-Herrero, A. M. Baró, N. Garcia, U. Landman, W. D. Luedtke, E. N. Bogachek and H.-P. Cheng, *Science*, 1995, **267**, 1793–1795.
3 Y. Cui, Q. Wei, H. Park and C. M. Lieber, *Science*, 2001, **293**, 1289–1292.
4 J.-M. Nhut, L. Pesant, J.-P. Tessonnier, G. Winé, J. Guille, C. Pham-Huu and M.-J. Ledoux, *Appl. Catal., A*, 2003, **254**, 345–363.
5 F. Wang and W. E. Buhro, *Small*, 2010, **6**, 573–581.
6 S. A. Johnson, D. Khushalani, N. Coombs, T. E. Mallouk and G. A. Ozin, *J. Mater. Chem.*, 1998, **8**, 13–14.
7 L. Cademartiri, R. Malakooti, P. G. O'Brien, A. Migliori, S. Petrov, N. P. Kherani and G. A. Ozin, *Angew. Chem., Int. Ed.*, 2008, **47**, 3814–3817.
8 R. Malakooti, L. Cademartiri, A. Migliori and G. A. Ozin, *J. Mater. Chem.*, 2008, **18**, 66–69.
9 I. Patla, S. Acharya, L. Zeiri, J. Israelachvili, S. Efrima and Y. Golan, *Nano Lett.*, 2007, **7**, 1459–1462.
10 K. H. Park, K. Jang, S. Kim, H. J. Kim and S. U. Son, *J. Am. Chem. Soc.*, 2006, **128**, 14780–14781.
11 L. Li, Y. Zhang, G. Li, X. Wang and L. Zhang, *Mater. Lett.*, 2005, **59**, 1223–1226.
12 Y.-W. Jun, J.-S. Choi and J. Cheon, *Angew. Chem., Int. Ed.*, 2006, **45**, 3414–3439.
13 Z. Liu, D. Xu, J. Liang, J. Shen, S. Zhang and Y. Qian, *J. Phys. Chem. B*, 2005, **109**, 10699–10704.
14 R. L. Penn and J. F. Banfield, *Geochim. Cosmochim. Acta*, 1999, **63**, 1549–1557.
15 K.-S. Cho, D. V. Talapin, W. Gaschler and C. B. Murray, *J. Am. Chem. Soc.*, 2005, **127**, 7140–7147.
16 P. Pyykkö and Y. Zhao, *Angew. Chem., Int. Ed. Engl.*, 1991, **30**, 604–605.
17 P. Pyykkö, J. Li and N. Runeberg, *Chem. Phys. Lett.*, 1994, **218**, 133–138.
18 K. W. Klinkhammer and P. Pyykko, *Inorg. Chem.*, 1995, **34**, 4134–4138.
19 Z. Huo, C.-K. Tsung, W. Huang, X. Zhang and P. Yang, *Nano Lett.*, 2008, **8**, 2041–2044.
20 X. Lu, M. S. Yavuz, H.-Y. Tuan, B. A. Korgel and Y. Xia, *J. Am. Chem. Soc.*, 2008, **130**, 8900–8901.
21 F. Wang, R. Tang, H. Yu, P. C. Gibbons and W. E. Buhro, *Chem. Mater.*, 2008, **20**, 3656–3662.
22 F. P. Bundy, *Phys. Rev.*, 1958, **110**, 314–318.
23 G. Schmid and B. Corain, *Eur. J. Inorg. Chem.*, 2003, 3081–3098.
24 Y. Li, J. Wang, Z. Deng, Y. Wu, X. Sun, D. Yu and P. Yang, *J. Am. Chem. Soc.*, 2001, **123**, 9904–9905.
25 B. Zhou, T. Ren and J. J. Zhu, *Int. J. Mod. Phys. B*, 2005, **19**, 2829–2834.
26 W. E. Morgan, W. J. Stec and J. R. Van Wazer, *Inorg. Chem.*, 1973, **12**, 953–955.
27 X. Liu, H. Cao and J. Yin, *Nano Res.*, 2011, **4**, 470–482.
28 C. J. Powell, *J. Electron Spectrosc. Relat. Phenom.*, 2012, **185**, 1–3.
29 C. Steinhagen, V. A. Akhavan, B. W. Goodfellow, M. G. Panthani, J. T. Harris, V. C. Holmberg and B. A. Korgel, *ACS Appl. Mater. Interfaces*, 2011, **3**, 1781–1785.
30 X. Lu and B. A. Korgel, *Chem. – Eur. J.*, 2014, **20**, 5874–5879.
31 X. Lu, K. J. Anderson, P. Boudjouk and B. A. Korgel, *Chem. Mater.*, 2015, **27**, 6053–6058.
32 Y.-H. Kim, Y.-W. Jun, B.-H. Jun, S.-M. Lee and J. Cheon, *J. Am. Chem. Soc.*, 2002, **124**, 13656–13657.
33 Y. Wang, J.-S. Kim, J. Y. Lee, G. H. Kim and K. S. Kim, *Chem. Mater.*, 2007, **19**, 3912–3916.
34 W. Yewu and S. K. Kwang, *Nanotechnology*, 2008, **19**, 265303.